Single-Channel Recording of TASK-3-like K$^+$ Channel and Up-Regulation of TASK-3 mRNA Expression after Spinal Cord Injury in Rat Dorsal Root Ganglion Neurons

Inseok Jang[2], Jun-Ho La[1], Gyu-Tae Kim[1], Jeong-Soon Lee[1], Eun-Jin Kim[1], Eun-Shin Lee[3], Su-Jeong Kim[4], Jeong-Min Seo[4], Sang-Ho Ahn[4], Jae-Yong Park[1], Seong-Geun Hong[1], Dawon Kang[1,†], and Jaehee Han[1,*]

[1]Medical Research Center for Neural Dysfunction and Departments of Physiology, [2]Thoracic Surgery, and [3]Rehabilitation Medicine, College of Medicine and Institute of Health Sciences, Gyeongsang National University, Jinju 660-751, [4]Yeungnam University Institute of Biomedical Engineering, Department of Rehabilitation Medicine, College of Medicine, Yeungnam University, Daegu 705-717, Korea

Single-channel recordings of TASK-1 and TASK-3, members of two-pore domain K$^+$ channel family, have not yet been reported in dorsal root ganglion (DRG) neurons, even though their mRNA and activity in whole-cell currents have been detected in these neurons. Here, we report single-channel kinetics of the TASK-3-like K$^+$ channel in DRG neurons and up-regulation of TASK-3 mRNA expression in tissues isolated from animals with spinal cord injury (SCI). In DRG neurons, the single-channel conductance of TASK-3-like K$^+$ channel was 33.0±0.1 pS at -60 mV, and TASK-3 activity fell by 65±5% when the extracellular pH was changed from 7.3 to 6.3, indicating that the DRG K$^+$ channel is similar to cloned TASK-3 channel. TASK-3 mRNA and protein levels in brain, spinal cord, and DRG were significantly higher in injured animals than in sham-operated ones. These results indicate that TASK-3 channels are expressed and functional in DRG neurons and the expression level is up-regulated following SCI, and suggest that TASK-3 channel could act as a potential background K$^+$ channel under SCI-induced acidic condition.

Key Words: Two-pore domain K$^+$ channel, Dorsal root ganglion, Spinal cord injuries, Acidosis

INTRODUCTION

Local tissue acidosis is usually accompanied by tissue injury, inflammation, and ischemia. After spinal cord injury (SCI), lactic acidosis occurs and metabolic acidosis exacerbates the spinal cord ischemic injury (Braughler and Hall, 1984; Farooque et al., 1996; Lang-Lazdunski et al, 2004). These processes are normally detected by sensory neurons. It is known that dorsal root ganglion (DRG) neurons, a collection of cell bodies of the afferent sensory fibers, participate in peripheral sensing of noxious stimuli. The peripheral noxious stimuli activate peripheral nociceptive transducer receptors and/or ion channels, and change the membrane potential of sensory DRG neurons. The excitability of DRG neurons is regulated in response to a number of pathological conditions (Rush et al, 2007).

DRG neurons express numerous ion channels, including acid-sensing ion channels (ASICs), transient receptor potential (TRP) cation channels (TRPV1 and TRPV4), ionotropic purinoceptor (P2X) ion channels, and acid-sensitive two-pore domain K$^+$ (K$_{2P}$) channels (Holzer, 2003; Kang et al., 2005; Kang and Kim, 2006; La et al., 2006). These channels are molecular sensors that detect noxious stimuli, in-cluding acidosis signals in DRG neurons under pathological conditions. Recent studies have been focused on identifying molecular sensors of acidosis (Holzer, 2003). ASICs and TRPV1 are directly activated by moderate and severe acidification, respectively, whereas P2X and K$_{2P}$ channels are indirectly regulated by acidosis through the modulation of cell membrane excitability (Holzer, 2003). In particular, K$_{2P}$ channels behave as background K$^+$ channels and are largely responsible for setting the resting membrane potential and suppressing neuronal excitation in response to acidosis-induced ASIC and TRP channel activity. Of the K$_{2P}$ channels, the mRNAs of TASK-1, TASK-2, TASK-3, TREK-1, TREK-2, TRAAK, and TRESK that are regulated by intracellular or extracellular acidosis are expressed (Kang and Kim, 2006); single-channel kinetics for TASK-2-like, TREK-1, TREK-2, TRAAK, and TRESK have also been described in DRG neurons (Kang et al., 2005; Kang and Kim, 2006; La et al., 2006). Single-channel recordings of TASK-1 and TASK-3, however, have not yet been made in DRG neurons, although their mRNAs are expressed in these cells and their activity appears in whole-cell currents (Cooper et al., 2004; Kang and Kim, 2006; Rau et al., 2006). Herein, we report that TASK-3-like K$^+$ channels are functionally expressed in rat neonatal DRG neurons, albeit at a very low level, and SCI increases the level of expression. These results suggest that TASK-3 channels may act as a potent

*Corresponding to: Jaehee Han, Department of Physiology, College of Medicine, Gyeongsang National University, 90 Chilam, Jinju, 660-751, Korea. (Tel) 82-55-751-8742, (Fax) 82-55-759-0169, (E-mail) jheehan@ gnu.ac.kr
†Co-corresponding author: dawon@gnu.ac.kr

ABBREVIATIONS: TASK, TWIK-Related acid sensitive K$^+$.

background K^+ channel in injured cells and tissues, regulating acid-related function under pathological conditions.

METHODS

Animal care

Sprague Dawley rats were purchased from Koatech Co. (Animal Breeding Center, Korea). Animal experiments were carried out in accordance with the guidelines of the Gyeongsang National University Animal Care and Use Committee (GLA-070827-R0047). Animals were housed under a 12-hr light/dark cycle in a pathogen-free area, with food and water freely available.

Spinal cord contusion injury animals

Female rats were used for efficient care and maintenance of SCI animals which suffer from neurogenic voiding dysfunction, because they have short urethras compared to males. The female rats (250 g, 12 weeks old, n=40) were deeply anesthetized with 3 mg/kg Rompun® (Bayer Korea, Seoul, Korea) and Zoletil50® (Virbac, Carros, France). Spinal contusion injury (n=15) was produced at the ninth thoracic spinal cord segment (T9) using the New York University (NYU) Impactor (New York, NY, USA). A 2.0 mm diameter rod was released from a 25 mm height onto the exposed spinal cord. Sham-operated animals (n=15) underwent the same operation as the animals with SCI, except for the contusion with the impactor. After SCI or sham surgery, the overlying muscles and skin were closed in layers with 4.0 silk sutures. The animals were then allowed to recover on a heating pad. To prevent urinary tract infection, Fortecillin comp (penicillin streptomycin HCl, Bayer Korea, Seoul, Korea) was administered twice a day at a dose of 20,000 IU/kg after operation. Bladders were manually emptied twice a day until the bladder-emptying reflex returned (typically within nine days after the injury).

Basso-Beattie-(BBB) locomotor scoring

The BBB test (Basso et al., 1995), a behavioral test, was performed to measure the recovery of hind-limb function after spinal cord contusion. Briefly, rats adapted to the open-field (1.5×0.6 m) used for the test were allowed to continuously walk around in the open-field for 4 min. Hind-limb function was assigned a score ranging from a minimum of 0 (no observable movement) to a maximum of 21 (normal locomotion). The test was performed four weeks post-SCI.

Isolation of dorsal root ganglion (DRG) and culture of DRG neurons

DRGs adjacent to the ninth thoracic spinal cord segment (T9) were dissected from sham-operated and SCI animals. DRGs for culture were dissected from both levels of the thoracic and lumbar spinal cord of neonatal rats (postnatal day 1 or day 2, P1-2). A total of 35 rats were used in this study. Cultured DRG neurons were prepared as described previously (Oh et al., 1996). Briefly, ganglia dissected from both levels of the thoracic and lumbar spinal cord of P1-2 rats were collected in cold (4°C) Dulbecco's modified Eagles' medium (DMEM) containing 10% FBS (Invitrogen, Grand Island, NY), 1 mM sodium pyruvate, 25 ng/ml nerve growth factor, 10 U/ml penicillin (Invitrogen), and 10 μg/ml streptomycin (Invitrogen). Ganglia were washed three times with DMEM and incubated for 30 min in DMEM containing 1 mg/ml collagenase (Type II; Worthington, Freehold, NJ, USA). The ganglia were then washed three times with Mg^{2+}-and Ca^{2+}-free Hank's Balanced Salt Solution (HBSS) and incubated with gentle shaking in warm (37°C) HBSS containing 2.5 mg/ml trypsin (Invitrogen). The solution was centrifuged at 1,000 rpm (194 g) for 10 min, and the pellet was washed three times with DMEM containing 10% FBS to inhibit the enzyme action. The pellet was suspended in culture medium and gently triturated with a heat-polished Pasteur pipette. The suspension was plated on glass coverslips coated with poly- L- lysine and placed in a culture dish. Neurons were incubated at 37°C in a 95% air-5% CO_2 gas mixture. Cells were used 1~5 days after plating.

Reverse transcriptase-polymerase chain reaction (RT-PCR) analysis

Total RNA was isolated from neonatal and adult DRGs, spinal cord, and brain using TRIzol Reagent (Invitrogen). First-strand cDNAs were synthesized from total RNA isolated from DRGs, spinal cord, and brain using oligo (dT) (RT-andGO Mastermix, Qbiogene, Cambridge, UK) and then used as a template for PCR amplification. Specific primers for each K_{2P} channel were used in PCR reactions with *Taq* polymerase (G-Taq™, Cosmo Genetech, Seoul, Korea). Table 1 lists the DNA sequences of the primers used to detect the expression of K_{2P} channels. PCR was conducted in a final reaction volume of 30 μl containing 1 μl (~50 ng) of diluted first-strand cDNA. PCR conditions included an initial denaturation at 94°C for 5 min, followed by 30 cycles at 94°C for 30 s, 57°C for 45 s, and 72°C for 45 s, and a final extension step at 72°C for 10 min. The PCR products were directly sequenced with the ABI PRISM® 3100-Avant Genetic Analyzer (Applied Biosystems, CA, USA).

Real-time PCR analysis

Changes in TASK-3 mRNA expression in the brain, spinal cord, and DRG following SCI were quantified using real-time PCR with FastStart DNA Master SYBR Green I (Roche Applied Science, Mannheim, Germany) and the LightCycler System (LightCycler 2.0 instrument, Roche). TASK-3 mRNA expression was normalized to that of glyceraldehyde-3-phosphate dehydrogenase (GAPDH). Real-time PCR primers were designed using Genscript (https://www.genscript. com/ssl-bin/app/primer). The following primers were used to specifically amplify TASK-3 (GenBank accession number AF192366): [5'- TGACTACTATAGGGT TCGGCG-3' (sense) and 5'-AAGTAGGTGTTCCTCAGCA CG-3' (anti-sense)]. The primers used to amplify GAPDH (GenBank accession number NM_017008) were [5'-CTAA AGGGCATCCTGGGC-3' (sense) and 5'-TTACTCC TTGGA GGCCATG-3' (anti-sense)]. PCR conditions consisted of a denaturing cycle (95°C for 10 min), 40 cycles of PCR (95°C for 7 s, 56°C for 7 sec, and 72°C for 10 sec), a melting cycle (65°C for 60 sec), a step cycle (increase from 65°C to 95°C at a rate of 0.1°C/sec), and a cooling step (40°C for 30 sec). Melt-curve analysis was conducted to confirm that each product was produced, and correct product size was confirmed on a 1.5% agarose gel.

Table 1. Primer sequences used for RT-PCR and real-time PCR

Name (Channel)	Primer sequences (5' to 3')	GenBank accession nos.	Expected size (bp)
GAPDH	Forward: CTAAAGGGCATCCTGGGC Reverse: TTACTCCTTGGAGGCCATG	**NM_017008**	201
	(Real-time PCR) Forward: CATGGCCTTCCGTGTTC Reverse: CTGCTTCACCACCTTCTT		103
KCNK3 (TASK-1)	Forward: TGTTCTGCATGTTCTACGCG Reverse: TGGAGTACTGCAGCTTCTCG	**NM_033376**	702
KCNK5 (TASK-2)	Forward: TGGTAATGTGGCTCCCAAGA Reverse: CAAAGCCAATGGTGGAGATG	**AM229406**	441
KCNK9 (TASK-3)	Forward: TGACTACTATAGGGTTCGGCG Reverse: AAGTAGGTGTTCCTCAGCACG	**AF192366**	517
	(Real-time PCR) Forward: GAAGTTTCTATGGAGAACATGGTGA Reverse: CGTGGAAGAAGCTCCAAT		105
KCNK2 (TREK-1)	Forward: TGCCAAAGTGGAGGACACAT Reverse: CTCTCCCACCTCTTCCTTCG	**AF325671**	361
KCNK10 (TREK-2)	Forward: CAGCCCAAGAGTGCCACTAA Reverse: GGATCCCAAAGATGGCGTAT	**NM_023096**	493
KCNK4 (TRAAK)	Forward: CACCACTGTAGGCTTTGGCGATTATG Reverse: ACTCTGCGTGTCTGAGGACTCGTCG	**NM_053804**	445
KCNK18 (TRESK)	Forward: CCAGAAGCAGAGGAGAACCC Reverse: CTGCACCAGCATCAATGACA	**AY567970**	475

Western blot analysis

Rat DRG was homogenized in a lysis buffer containing 50 mM HEPES (pH 7.5), 150 mM NaCl, 10% glycerol, 100 mM NaF, 0.2 mM Na-orthovanadate, 0.5% NP-40, 1.5 mM $MgCl_2$, 1 mM EGTA, 1 mM dithiothreitol, 1 g/ml leupeptin, 10 mM benzamidine, 1 g/ml pepstatin A, 1 mM phenyl-methylsulfonyl fluoride, and 10.5 g/ml aprotinin, and incubated for 20 min on ice with intermittent vortexing. Extracts were clarified by centrifugation at 14,000 rpm (19,300 g) for 15 min at 4°C. The resulting supernatant was separated with 10% SDS-polyacrylamide gel and transferred to nitro-cellulose membrane for 30 min using semi-dry transfer (Bio-Rad, CA, SUA). The membranes were blocked with 5% fat-free dry milk and then incubated with TASK-3 polyclonal antibody (1 : 500 dilutions, Chemicon, CA, USA) and β-actin polyclonal antibody (1 : 1,000 dilutions, Sigma, MO, USA). These were followed by incubation with a secondary peroxidase-conjugated anti-rabbit antibody at 1 : 2,000 (Sigma, MO, USA). Immuno-positive bands were visualized by enhanced chemiluminescence (ECL Plus kit, ELPIS, Taejon, Korea) following manufacturer's instructions.

Electrophysiological studies

Electrophysiological recording was performed using a patch clamp amplifier (Axopatch 200, Axon Instruments, Union City, CA). Single-channel currents were digitized with a digital data recorder (VR10, Instrutech, Great Neck, NY) and stored on videotape. The recorded signal was filtered at 2 kHz using an 8-pole Bessel filter (-3 dB; Frequency Devices, Haverhill, MA) and transferred to a computer (Samsung) using the Digidata 1320 interface (Axon Instruments, Union City, CA) at a sampling rate of 20 kHz. Threshold detection of channel openings was set at 50%. Single channel currents were analyzed with the pCLAMP program (version 9, Axon). The filter dead time was 100 μs (0.3/cutoff frequency) for single channel analysis, therefore, events lasting less than 50 μs were not detected. Data were analyzed to obtain a duration histogram, amplitude histogram, and a description of channel activity (NP_o, where N is the number of channels in the patch and P_o is the probability of a channel being open). NP_o was determined from ~1~2 min of current recording. The single-channel current tracings shown in the figures were filtered at 2 kHz. In experiments using cell-attached patches and excised patches, the pipette and bath solutions contained (mM): 150 KCl, 1 $MgCl_2$, 5 EGTA, and 10 HEPES (pH 7.3). The pH was adjusted to desired values with HCl or KOH. All other chemicals were purchased from Sigma Chemical Co. (St Louis, MO, USA) unless otherwise stated.

Statistics

Light Cycler Software 4.0 (Roche, Mannheim, Germany) was used to capture real-time PCR data. LAS-4000 (Fujifilm corp, Tokyo, Japan), a luminescent image analyzer, captures images of agarose and Western blot. The bands obtained from PCR and Western blot were quantified by Sigma Gel image analysis software (version 1.0, Jandel Scientific, CA, USA) and Quantity One software (version 4.6.3) attached to GS-800 Calibrated densitometer (Bio-Rad. CA, USA). Relative mRNA and protein levels were calculated by referring them to the amount of GAPDH and

β-actin, respectively. Student's *t*-test was used with $p < 0.05$ or < 0.01 defined as the criterion for significance. Data are represented as mean±S.D. unless otherwise specified.

RESULTS

Functional expression of pH-sensing K_{2P} channels in DRG neurons

Single-channel recordings were performed in rat neonatal (P1-2) DRG neurons ranging from 10 to 38 μm in diameter. Fig. 1A shows a photomicrograph of rat P1 DRG neurons of various diameters cultured on glass cover-slips. The DRG neurons isolated from P1-2 rats were cultured for two days in medium containing nerve growth factor (NGF, 25 ng/ml). As shown in Fig. 1B, RT-PCR data showed that DRG express the mRNAs of TASK-1, TASK-2, TASK-3, TREK-1, TREK-2, TRAAK, and TRESK, in agreement with earlier studies (Medhurst et al., 2001; Kang et al., 2005; Kang and Kim, 2006). These channels in DRG neurons were functionally expressed and regulated by changes in intracellular or extracellular pH (pH_i or pH_o) (Fig. 1C). At $+60$ and -60 mV, the single-channel conductances of the various channels studied were as follows: TRESK (14 pS and 15 pS), TASK-2-like (37 pS and 80 pS), TREK-1 (112 pS and 120 pS), TREK-2 (50 pS and 138 pS), and TRAAK (73 pS and 120 pS). The activities of TRESK and TASK-2-like K^+ channels were inhibited by extracellular acidosis, whereas those of TREK-1 and TREK-2 were activated by intracellular acidosis. In contrast, however, TRAAK was activated when intracellular pH was increased from 7.3 to 8.3 (Fig. 1C).

Expression of TASK-3-like K^+ channels in DRG neurons

TASK-1 and TASK-3 mRNAs were detected in DRG neurons (Fig. 1B). A hallmark of TASK-1 and TASK-3 channels is their sensitivity to pH_o. To identify whether TASK-1 and TASK-3 are expressed in neonatal rat DRG neurons, single-channel recording was performed in DRG neurons. From 420 cell-attached patches, TASK-3-like K^+ channel was observed in some patches (2.9%, 12 of 420 patches studied). The K^+ selectivity of TASK-3-like channels was confirmed when the expected shift in reversal potential from
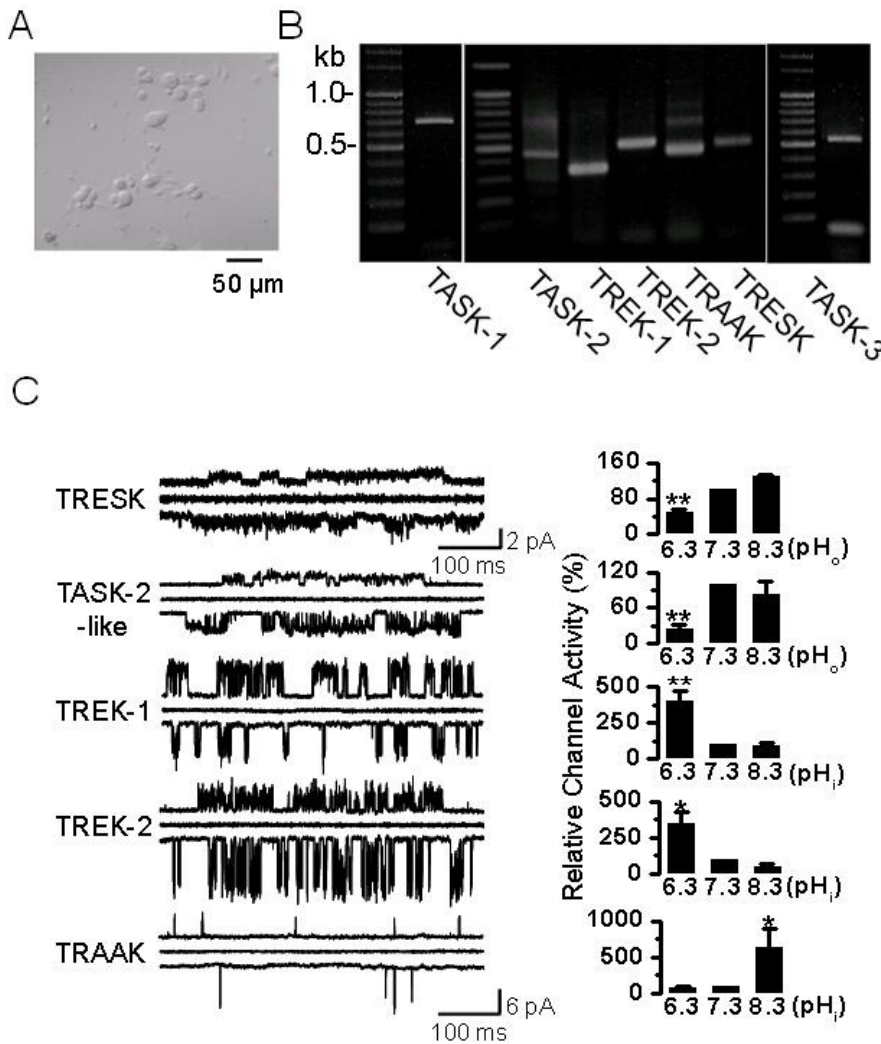

Fig. 1. pH sensitive background K^+ channels in DRG neurons. (A) Photomicrograph of DRG neurons cultured for two days in medium containing NGF. These neurons were isolated from postnatal day 1 or 2 (P1-2) rats. Scale bar, 50 μm. (B) The expression of K_{2P} channel mRNA. In the P1~2 rat DRG, PCR products of TASK-1 (702 bp), TASK-2 (441 bp), TASK-3 (517 bp), TREK-1 (361 bp), TREK-2 (493 bp), TRAAK (445 bp), and TRESK (475 bp) were obtained and confirmed by sequencing. (C) Cell-attached patches were formed on DRG neurons, and single-channel openings were recorded at $+60$ mV and -60 mV at room temperature. Pipette and bath solutions contained 150 mM KCl. Representative traces show five types of single-channel current at $+60$ mV (upper trace), 0 mV (middle), and -60 mV (lower). The horizontal scale bar indicates 100 ms. The vertical scale bar indicates 2 pA for TRESK and 6 pA for other channels. Bar graphs show the pH sensitivity of each channel (mean±SE, n=4~6). *$p < 0.05$ and **$p < 0.01$ compared to the corresponding control (pH 7.3).

0 to -40 ± 3 mV was observed in outside-out patches when extracellular K^+ concentration changed from 150 mM to 30 mM. Outward channel activity was dramatically decreased when K^+ in the bath was replaced with Na^+ (n=3). The channels were active at all membrane potentials tested ($+80$ to -80 mV, Fig. 2A).

Although five other types of background K^+ channels were present in DRG neurons, they all showed different single-channel conductances and kinetics (Fig. 1C). Figure 2A showed the single-channel opening of TASK-3-like K^+ channels at different membrane potentials in cell-attached patches. The mean open time and the current-voltage relationship of this K^+ channel, determined from duration and amplitude histograms, were similar to those of cloned TASK-3 expressed in COS-7 cells. In DRG neurons, TASK-3-like K^+ channel activity was decreased after the formation of inside-out patches but did not change over time or in response to voltage changes, indicating that TASK-3-like K^+ channels function as background K^+ channels. The single-channel conductance of TASK-3 was 33.0 ± 0.1 pS at -60 mV and 17.5 ± 0.1 pS at $+60$ mV. However, TASK-3-like K^+ channels in DRG neurons showed slightly lower single-channel conductance and shorter mean open time at -60 mV than the same cloned channels expressed in COS-7 cells, indicating that the currents may be masked by many kinds of channels, and that other molecules may be func-

tioning concurrently with the TASK-3-like channels in vivo.

To study the properties of this K^+ channel in more detail, outside-out patches containing only TASK-3-like K^+ channels were formed on DRG neurons. Based on their mean open times (~0.5 ms), single-channel conductance, and their weak inwardly rectifying current-voltage relationship (Figs. 2A to 2C), we identified these channels. The pH sensitivity of each channel was analyzed by measuring channel activity at different pH_o values. TASK-3-like K^+ channels were inhibited by $65\pm5\%$ when pH was lowered from 7.3 to 6.3 in outside-out patches. The inhibition of channel activity at pH_o 6.8 and 6.3 was not significantly different, but the channel activity at pH_o 6.8 was higher than at pH_o 6.3 (Fig. 2D). Single-channel kinetics, pH-sensitivity, and mRNA expression suggest that TASK-3 may be the molecular signature of TASK-3-like K^+ channels in DRG neurons.

Changes in TASK-3 mRNA and protein expression levels after spinal cord injury

Changes in TASK-3 mRNA and protein expression were analyzed in adult animals following a 25-mm contusion SCI to the T9 spinal cord segment. The SCI animal model designed by contusion can mimic the majority of pathologies related to neuronal injury, including acidosis. Using the BBB locomotor rating scale, open-field motor function was
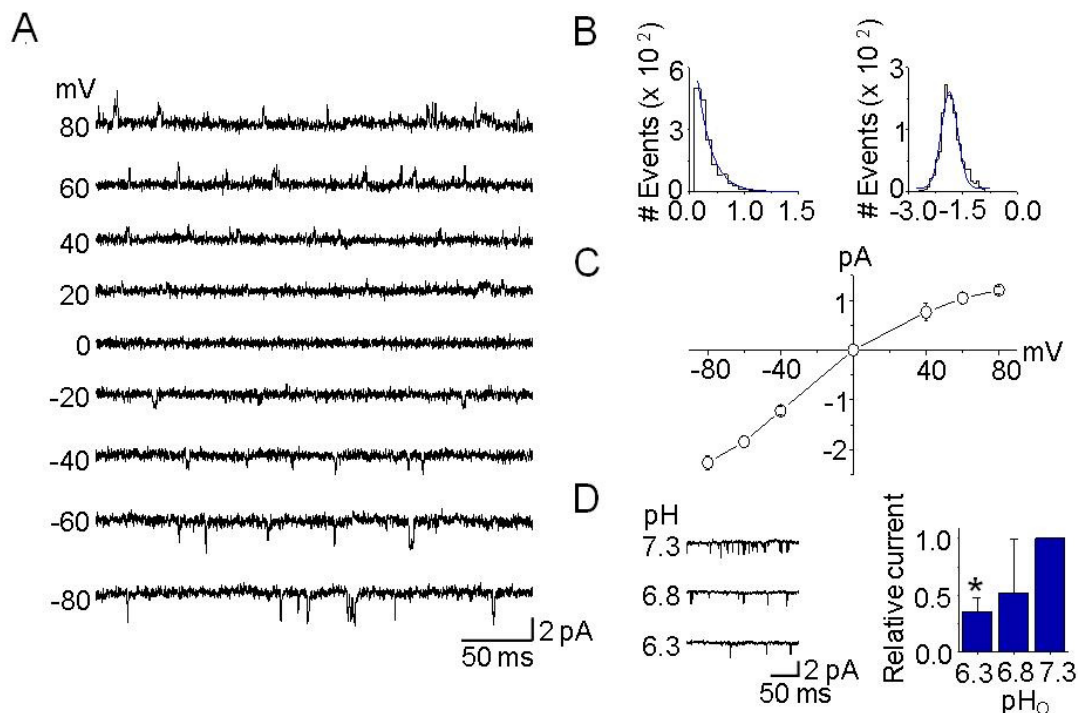

Fig. 2. Single-channel kinetics of TASK-3-like K^+ channels in DRG neurons. (A) Cell-attached patches were formed, and single-channel openings were recorded at the different membrane potentials, noted on the left. Pipette and bath solutions contained 150 mM KCl. (B) Histograms of open time duration (left) and amplitude (right) of TASK-3-like K^+ channel were obtained from openings at -60 mV. They were fitted by single exponential and Gaussian functions, respectively. (C) Single-channel amplitudes were determined from the amplitude histogram for each membrane potential in order to construct the current-voltage relationship. Each point represents mean±SD of four repeated experiments. (D) The pH_o sensitivity of single-channel currents from TASK-3-like K^+ channels in DRG neurons. Single-channel currents from outside-out patches are shown as inward currents recorded at -60 mV when KCl concentration was 150 mM on both sides of the patch. Typical channel openings from three independent experiments are shown. The bar graph shows the effects of pH_o changes on TASK-3-like K^+ channel activity. Each bar represents mean±SD of three repeated experiments. The asterisk indicates significant difference from the control value at pH 7.3 ($p<0.05$).
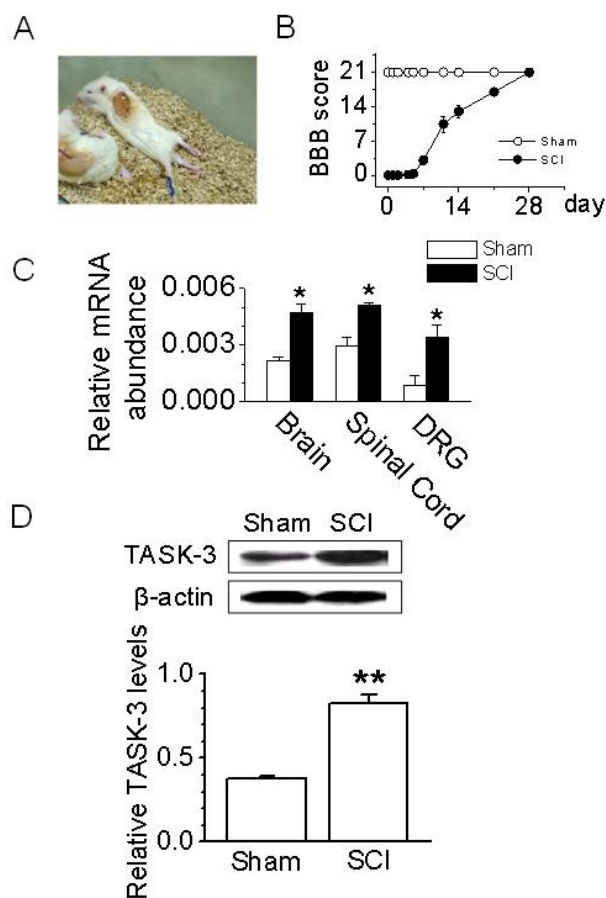
Fig. 3. Up-regulation of TASK-3 mRNA and protein expression after spinal cord injury. (A) A photograph of rats with a T9 spinal segment injury. These rats exhibited paralysis of the hind legs. (B) The BBB open-field locomotor rating scores show spontaneous partial recovery of motor function after SCI (n=10 animals per group). Data points represent mean±SD. (C) Changes in TASK-3 mRNA expression in SCI animals. PCR was conducted on cDNA templates obtained from brain, spinal cord, and DRG of SCI and sham-operated animals at 48 hours after injury. The bar graph summarizes the levels of TASK-3 mRNA expression which changed after SCI. Each bar represents mean±SD of three repeated experiments. Asterisks indicate significant difference from the corresponding control value (sham-operated groups, p < 0.05). (D) Western blot analysis in DRG. TASK-3 protein level increased in DRG obtained from SCI animal at 48 hours after injury. The bar graph shows the up-regulation of TASK-3 protein expression in DRG obtained from SCI animals. Each bar represents mean±SD of three repeated experiments. Asterisks (**) indicate significant difference from the corresponding control value (sham-operated groups, p < 0.01).

assessed after injury. Following SCI, rats showed paralysis (Fig. 3A), though they spontaneously recovered extensive movement of both hind limbs. The BBB score was 20±2 at 28 days (Fig. 3B).

To quantify the changes in expression of the TASK-3 channel after SCI, real-time PCR and Western blot analysis were performed in the brain, spinal cord, and DRG harvested at 48 hrs after SCI. The mRNA expression levels of the TASK-3 channel in the brain, spinal cord, and DRG were ~2-fold higher in injured animals than in sham-oper-

ated animals (Fig. 3C). In DRG, TASK-3 protein level was significantly increased (by 2.2-fold) in injured animals (p < 0.01). All results were normalized to the expression of GAPDH mRNA and β-actin protein (Fig. 3C and Fig. 3D).

DISCUSSION

In the present study, we studied for the first time the single-channel kinetics of TASK-3-like K⁺ channels in neonatal rat DRG neurons and observed the up-regulation of TASK-3 mRNA and protein expression in response to aging and SCI. These findings suggest that TASK-3 may play an important role in the regulation of cellular excitability during injury-induced pathology.

Expression of pH-sensitive background K⁺ channels in DRG neurons

TREK-1, TREK-2, TRAAK, TRESK, and TASK-2- and TASK-3-like K⁺ channels are functionally expressed in P1-2 rat DRG neurons. The activity of these channels is known to be modulated by changes in pH. TASK-2, TASK-3, and TRESK are inhibited by low pH_o (Kang et al., 2004a; Kang and Kim, 2004; Kang et al., 2004b), whereas TREK-1 and TREK-2 are activated by low pH_i (Kim, 2003; Kang et al., 2005), and TRAAK is activated by alkaline pH_i (Kim, 2003). The pH sensitivity of these channels suggests that these channels function together with other acid-sensitive channels in pathologies involving acidosis.

The negative resting membrane potential of DRG neurons (−60 mV) (Zhang et al., 2003) is likely to be the net effect of both inward TRP and ASICs currents and outward K⁺ currents which are larger than inward currents. K_{2P} channels are expected to play an active role in the regulation of DRG neuron excitability. In the present study, TASK-3-like K⁺ channels were recorded in P1~2 DRG neurons at low levels, suggesting that TASK-3-like K⁺ channels do not provide a significant background K⁺ current, at least in the cultured P1~2 DRG neurons used in this study. In DRG neurons from adult rat, small TASK-like K⁺ currents were recorded at the whole-cell level (Rau et al., 2006), indicating that TASK expression may be higher in adult DRG neurons than in neonatal neurons. This idea is supported by our data showing that TASK-3 mRNA expression was higher in adult DRG (data not shown).

Up-regulation of TASK-3 expression in response to spinal cord injury

In addition to aging, injury induces changes in TASK-3 expression. After injury or constriction, quiescent neurons begin to fire, reflecting hyperexcitability of DRG neurons. The firing activity travels into the spinal posterior horn and eventually to the higher central nervous system. This leads to central pain sensitization. Intense noxious stimuli to nerves and tissues can increase the excitability of nociceptive neurons in the spinal cord and cause the release of unsaturated free fatty acids. In addition, changes in pH and temperature as well as edema lead to a negative mechanical stretch, which can modulate various ion channels (Smith, 2006).

The role of K⁺ channels in posttraumatic axonal dysfunction has extensively been examined pharmacologically. Nevertheless, relatively little is known about the changes

in the expression of K^+ channels following acute or chronic SCI. Moreover, changes in K_{2P} channel expression after SCI have not yet been reported. In this study, the expression of TASK-3 channel was up-regulated after SCI. TASK-3 channels are expected to play more active roles in modulating DRG neuron excitability under SCI-induced pathological conditions than they do under physiological conditions. If the pathological condition induces acidosis, TASK-3 channels will be inhibited; Inhibition of TASK-3 channel is likely to induce cell excitability. This contrasts with the common notion that K_{2P} channels function to suppress cell excitability. However, up-regulation of TASK-3 expression probably plays a more important role in K^+ homeostasis and regulation of resting membrane potential in response to SCI than it does under normal conditions, because SCI induces a complex array of *in vivo* changes. The induction of DRG neuron hyperexcitability in the SCI model is accompanied by reduction in potassium currents. It is unclear whether changes in TASK-3 expression counteract or promote the pathology induced by SCI. Therefore, the characteristics of TASK-3 channels in DRG neurons isolated from SCI animals should be studied in future by whole-cell or single-channel recording, and such recordings should examine the membrane potential, channel activity, current-voltage curve, unitary conductance, and ion channel kinetics for comparison to normal DRG neurons. Finally, the functions of these channels in the higher central nervous system, such as the spinal cord, hippocampus, and cerebral cortex should be investigated.

ACKNOWLEDGEMENTS

REFERENCES

Basso DM, Beattie MS, Bresnahan JC. A sensitive and reliable locomotor rating scale for open field testing in rats. *J Neurotrauma* 12: 1−21, 1995

Braughler JM, Hall ED. Effects of multi-dose methylprednisolone sodium succinate administration on injured cat spinal cord neurofilament degradation and energy metabolism. *J Neurosurg* 61: 290−295, 1984

Cooper BY, Johnson RD, Rau KK. Characterization and function of TWIK-related acid sensing K^+ channels in a rat nociceptive cell. *Neuroscience* 129: 209−224, 2004

Farooque M, Hillered L, Holtz A, Olsson Y. Effects of methylprednisolone on extracellular lactic acidosis and amino acids after severe compression injury of rat spinal cord. *J Neurochem* 66: 1125−1130, 1996

Holzer P. Acid-sensitive ion channels in gastrointestinal function. *Curr Opin Pharmacol* 3: 618−625, 2003

Kang D, Choe C, Kim D. Thermosensitivity of the two-pore domain K^+ channels TREK-2 and TRAAK. *J Physiol* 564: 103−116, 2005

Kang D, Han J, Talley EM, Bayliss DA, Kim D. Functional expression of TASK-1/TASK-3 heteromers in cerebellar granule cells. *J Physiol* 554: 64−77, 2004a

Kang D, Kim D. Single-channel properties and pH sensitivity of two-pore domain K^+ channels of the TALK family. *Biochem Biophys Res Commun* 315: 836−844, 2004

Kang D, Kim D. TREK-2 (K_{2P}10.1) and TRESK (K_{2P}18.1) are major background K^+ channels in dorsal root ganglion neurons. *Am J Physiol Cell Physiol* 291: C138−146, 2006

Kang D, Mariash E, Kim D. Functional expression of TRESK-2, a new member of the tandem-pore K^+ channel family. *J Biol Chem* 279: 28063−28070, 2004b

Kim D. Fatty acid-sensitive two-pore domain K^+ channels. *Trends Pharmacol Sci* 24: 648−654, 2003

La JH, Kang D, Park JY, Hong SG, Han J. A novel acid-sensitive K (+) channel in rat dorsal root ganglia neurons. *Neurosci Lett* 406: 244−249, 2006

Lang-Lazdunski L, Bachet J, Rogers C. Repair of the descending thoracic aorta: impact of open distal anastomosis technique on spinal cord perfusion, neurological outcome and spinal cord histopathology. *Eur J Cardiothorac Surg* 26: 351−358, 2004

Medhurst AD, Rennie G, Chapman CG, Meadows H, Duckworth MD, Kelsell RE, Gloger, II, Pangalos MN. Distribution analysis of human two pore domain potassium channels in tissues of the central nervous system and periphery. *Brain Res Mol Brain Res* 86: 101−114, 2001

Oh U, Hwang SW, Kim D. Capsaicin activates a nonselective cation channel in cultured neonatal rat dorsal root ganglion neurons. *J Neurosci* 16: 1659−1667, 1996

Rau KK, Cooper BY, Johnson RD. Expression of TWIK-related acid sensitive K^+ channels in capsaicin sensitive and insensitive cells of rat dorsal root ganglia. *Neuroscience* 141: 955−963, 2006

Rush AM, Cummins TR, Waxman SG. Multiple sodium channels and their roles in electrogenesis within dorsal root ganglion neurons. *J Physiol* 579: 1−14, 2007

Smith GT. Pharmacological characterization of ionic currents that regulate high-frequency spontaneous activity of electromotor neurons in the weakly electric fish, Apteronotus leptorhynchus. *J Neurobiol* 66: 1−18, 2006

Zhang XF, Gopalakrishnan M, Shieh CC. Modulation of action potential firing by iberiotoxin and NS1619 in rat dorsal root ganglion neurons. *Neuroscience* 122: 1003−1011, 2003